RESEARCH PAPER

Evaluating The Cytotoxic Effects Of Silver Nanoparticles Derived From *Pogostemon Benghalensis* Brum. F. Kunth. Extract On A549 Lung Cancer Cells

T. Manikandan[1], G. Jeevanantham[2], K. Vignesh[3], A. Thirumurugan[3*], A. Lakshmi Prabha[1*]

[1*]Department of Botany, School of Life Science, Bharathidasan University, Tiruchirappalli-620 024.

[2]Department of Botany, Thanthai Hans Roever College (Autonomous) (Affiliated to Bharathidasan University, Tiruchirappalli), Perambalur - 621 220, Tamil Nadu, India.

[3*]Reproductive Endocrinology Lab, Department of Research, Saveetha College of Nursing (SCON), Saveetha Institute of Medical and Technical Sciences (SIMATS), Thandalam, Chennai, Tamil Nadu 602105, India

ABSTRACT

This study examines the green synthesis, characterisation, and bioactivity of silver nanoparticles (AgNPs) produced from *Pogostemon benghalensis* extract. A clear change in color from pale yellow to deep brown showed that nanoparticles were formed. FTIR research showed that there were alcohols, phenols, carboxylic acids, and amine groups that helped reduce and stabilize AgNPs. The UV–Vis spectra showed a strong SPR peak at 440 nm, and the XRD data showed that AgNPs had a crystalline, face-centered cubic structure. The DLS test showed that the z-average particle size was 113.6 nm and the PDI was 0.262. The zeta potential test showed that the nanoparticles were weakly charged but stable. SEM micrographs showed particles that were round or almost spherical and showed signs of minor aggregation. EDX analysis confirmed that silver was the main element. The biosynthesized AgNPs shown significant antibacterial efficacy against E. coli, S. aureus, B. subtilis, and V. cholerae, with V. cholerae exhibiting the greatest sensitivity. Antioxidant research showed that the ability to scavenge free radicals depended on the concentration, with high IC_{50} values for DPPH, H_2O_2, and phosphomolybdenum tests. Research on the cytotoxicity of A549 lung cancer cells showed that the drug worked better at higher doses, with an IC_{50} of 47 µg/mL. AO/EtBr dual labeling indicated cell death caused by apoptosis, which was shown by chromatin condensation, nuclear fragmentation, and orange-red fluorescence in the treated cells. In general, AgNPs made with P. benghalensis showed promise as antimicrobials, antioxidants, and anticancer agents.

Keywords: Green synthesis; *Pogostemon benghalensis*; Silver nanoparticles; FTIR; XRD; UV–Vis; Antibacterial activity; Antioxidant activity; Cytotoxicity; A549 cells; Apoptosis.

How to cite this article: Manikandan T, Jeevanantham G, Vignesh K, Thirumurugan A, Lakshmi Prabha A., Evaluating The Cytotoxic Effects Of Silver Nanoparticles Derived From Pogostemon Benghalensis Brum. F. Kunth. Extract On A549 Lung Cancer Cells. Int J Drug Deliv Technol. 2026;16(45s): 1232-1251; DOI: 10.25258/ijddt.16.45s.126

Source of support: Nil

Conflict of interest: None

1. INTRODUCTION

Nanotechnology, especially the creation of metal-based nanoparticles, has become a quickly growing subject with the power to change biomedical research. Among these, silver nanoparticles (AgNPs) have gained exceptional attention because of their remarkable physicochemical properties, including a high surface-area-to-volume ratio, strong surface plasmon resonance (SPR), and the ability to exhibit potent biological activities across antimicrobial, antifungal, antiviral, antioxidant, and anticancer domains (Muthukrishnan et al., 2025; Singaravelu et al., 2025). AgNPs have a number of biological effects that work together, such as making reactive oxygen species (ROS) inside cells, breaking down membranes, changing the balance of redox homeostasis in cells, damaging mitochondria, and releasing Ag^+ ions that interact with biomolecules. These systems together stop microbial and cancer cells from growing or cause them to die on purpose. Conventional chemical and physical techniques for synthesizing AgNPs sometimes depend on perilous reducing chemicals, elevated temperatures, or complex instrumentation, which raises issues regarding environmental safety, cytotoxic impurities, and scalability (Hosny et al., 2025). These kinds of problems led to the creation of green synthesis methods. Using plant extracts, microbial cultures, or other biological systems to make nanoparticles in a green (biogenic) way has become a

sustainable, non-toxic, and cost-effective option. Plant-mediated synthesis is especially useful since phytochemicals like flavonoids, phenolics, alkaloids, tannins, saponins, and terpenoids may all work together to reduce, stabilize, and cap things at the same time. This makes the process both easy and good for the environment. Recent reviews emphasize the swift proliferation of plant-based AgNP synthesis and its biological applications, highlighting the benefits of mild reaction conditions, improved biocompatibility, and enhanced functional surface chemistry provided by phytochemical capping agents (Kulkarni et al., 2023; Chandraker et al., 2024). The biogenic nanoparticles that come from this process frequently have better colloidal stability, better biological interactions, and maybe selective anticancer capabilities since they have bioactive molecular coronas around them.

Plants in the genus Pogostemon (family Lamiaceae) are a rich source of phytochemicals that can be used in many different ways. Species from this genus are well-known for their antibacterial, antioxidant, anti-inflammatory, and wound-healing properties. These effects are due to the high levels of flavonoids, polyphenols, alkaloids, and essential oils they contain (Kumar et al., 2024; Jaishwal et al., 2024). Recent phytochemical studies have shown that Pogostemon benghalensis, in particular, has a lot of polyphenols, tannins, flavonoids, alkaloids, and saponin compounds that can help with bioreduction and stabilization of metal ions during nanoparticle synthesis (Dahiya et al., 2020). These phytochemicals not only help nanoparticles develop, but they also affect their size, shape, crystallinity, and bioactivity (Pirsaheb et al., 2024; Singh et al., 2023). Due to these characteristics, P. benghalensis has become a prospective option for the green synthesis of AgNPs with improved biological application. Prior research has documented the effective manufacture of AgNPs with aqueous or alcoholic extracts of P. benghalensis, then characterized through UV–Vis spectroscopy, FTIR, SEM imaging, and EDAX analysis (Begum et al., 2022).Although these investigations have shown that P. benghalensis-mediated AgNPs have excellent antimicrobial properties, there is still not much research on their ability to fight cancer, especially in human lung cancer models. By completing cytotoxicity testing and mechanistic investigations to fill this gap, the medicinal significance of these nanoparticles would be greatly enhanced (Sharma et al., 2024). The physicochemical characteristics of nanoparticles, including size, distribution, zeta potential, shape, and surface chemistry, are critical in influencing cellular uptake, biodistribution, biological activity, and toxicity (Yusuf et al., 2023). AgNPs from plants often have a phytochemical corona that makes them more stable in colloidal form and can change how they interact with cellular membranes and targets inside cells. Surface-bound phytochemicals may increase selectivity for cancer cells by causing ROS-dependent cell death while lowering toxicity to healthy cells. So, it is important to fully characterize nanoparticles employing methods including UV–Visible spectroscopy, SEM imaging, FTIR, DLS, and zeta potential testing. In addition to characterization, reliable cytotoxicity assays (MTT/WST), apoptosis analysis (AO/EtBr staining, Annexin V/PI), ROS quantification, and mitochondrial dysfunction markers are essential for determining anticancer potential and elucidating mechanistic insights (Eker et al., 2025; Sati et al., 2025).

Lung cancer is still one of the most common and deadliest types of cancer in the world, killing more than 1.8 million people each year (Balata et al., 2019; Roointan et al., 2019). Even though diagnostic imaging, targeted therapy, and immunotherapy have all improved, survival rates are still low because most people don't get diagnosed until the disease is advanced, the cancer spreads quickly, drugs don't work, and traditional chemotherapeutics are toxic to the body as a whole (Leiter et al., 2023; Bertolaccini et al., 2024). These difficulties show how important it is to find new treatments that work and are less harmful. The A549 human lung adenocarcinoma cell line, derived from type II alveolar epithelial cells, is extensively utilized as an in vitro model for screening novel anticancer agents due to its relevance to non–small cell lung cancer (NSCLC) biology and its appropriateness for mechanistic investigations (Pan et al., 2020; Wittlinger et al., 2021; Padinharayil et al., 2023). Consequently, assessing the cytotoxic and apoptotic effects of plant-mediated AgNPs on A549 cells can yield significant insights into their potential as anticancer agents (Ng et al., 2022; Wani et al., 2023; Barathi et al., 2024; Upadhyay et al., 2024).

Recent research indicates that biogenic AgNPs derived from various plant sources demonstrate considerable cytotoxicity against A549 cells, frequently through mechanisms involving ROS generation, apoptosis induction, mitochondrial impairment, and DNA fragmentation (Grewal et al., 2022; González-Vega et al., 2022; Adetunji et al., 2024; Ibrahim et al., 2025; Vidjeyamannane et al., 2025). Certain plant-derived AgNPs have exhibited low micromolar IC_{50} values, underscoring their potential as next-generation anticancer medicines (Jain et al., 2021). Nonetheless, discrepancies in synthesis conditions, inadequate mechanistic characterization, and restricted in vivo validation underscore the necessity for more systematic investigations to ascertain reliability and therapeutic significance (Mehta et al., 2025; Wankhede et al., 2025;Ayyadurai et al.,2022; Jeyaram et al.,2026). In this study, we present the green synthesis of silver nanoparticles utilizing *Pogostemon benghalensis* leaf extract, offer detailed physicochemical evaluation, and

assess their anticancer efficacy against A549 human carcinoma of the lung cells via cytotoxicity and apoptosis assays.

2. MATERIALS AND METHODS

2.1. Plant Collection and Identification

In March 2017, fresh leaves of *Pogostemon benghalensis* (Burm. f.) Kuntze were taken from Kolli Hills in Namakkal District, Tamil Nadu, India. The Botanical Survey of India (BSI) in Coimbatore recognized and confirmed the plant species taxonomically. They also kept a voucher specimen (Accession No. BSI/SRC/5/23/2021/Tech/99) for future reference. For documentation and verification purposes, a duplicate specimen was also kept in the High-Altitude Plant Section of the Department of Botany at Bharathidasan University in Tiruchirappalli, India.

2.2. Green Synthesis of Silver Nanoparticles (pb-AgNPs)

We cleaned fresh, healthy leaves of *Pogostemon benghalensis* under running water, dried them in the shade to keep the active phytoconstituents, and then crushed them into a fine powder. For 15 minutes, 100 mL of distilled water was heated with about 10 g of the powdered material. Whatman No. 1 filter paper was employed to filter the combination, and the extract that came out was used as a stabilizing and reducing agent. To make silver nanoparticles, 10 mL of plant extract was combined with 90 mL of 1 mM $AgNO_3$ solution and kept at room temperature in the dark to stop photoreduction. A visible color change from pale yellow to brown showed that silver nanoparticles were forming. The produced nanoparticles were collected using centrifugation at 12,000 × g for 15 minutes, thereafter washed 2–3 times with Milli-Q water to eliminate contaminants and unbound phytochemicals, and kept at 4 °C until further characterization, in accordance with the methodology outlined by (Kumara Swamy et al.2015).

2.2.3 Describing the AgNPs that were made

2.3. 1. Fourier Transform Infrared Spectroscopy (FTIR)

We used a Fourier Transform Infrared (FTIR) spectrometer to look at the functional groups in the synthesized sample between 4000 and 700 cm^{-1}. To make solid samples, the material was ground up with potassium bromide (KBr) and pressed into a clear pellet. To make liquid samples, thin films were deposited between KBr plates. Before analyzing the sample, a background spectrum was captured to get rid of any interference from the atmosphere. The spectra were taken at a resolution of 4 cm^{-1} and 32 scans. Characteristic absorption peaks were found to figure out which functional groups were responsible for reducing and stabilizing the nanoparticles.

2.3.2 UV–Visible Spectroscopy (UV–Vis)

To find out how much pure Ag+ ions are reduced, we look at the UV–Vis spectra of the reduction media in 1 ml of the samples and 1 ml of distilled water as a blank. We used a Perkin Elmer-Lambda 25 UV–vis spectrophotometer with a resolution of 1 nm from 300 to 800 nm to get a UV–vis spectrum of metallic silver.

2.3.3 XRD analysis (X-ray diffraction)

The crystalline dimensions and arrangement, phase nature, and lattice characteristics of the green synthesized AgNPs were evaluated using the XRD method (Bruker D8 advance model) and the radiation spectrum of Cu-K, with a scattering 2θ range of 20° – 80°. The instrument operated at 30 kV with a current of 30 mA (Narayanan, et al., 2021).

2.3.4 Dynamic Light Scattering (DLS)

Using a Dynamic Light Scattering (DLS) equipment, we examined the hydrodynamic size, size distribution, and zeta potential of the nanoparticles we made. A little amount of the nanoparticle sample was mixed with deionized water and then sonicated to make a homogeneous suspension. We put the suspension in a cuvette and took measurements at room temperature. The equipment looked at changes in the intensity of scattered light to figure out the average particle size, polydispersity index (PDI), and zeta potential. This gave information about how stable and dispersed the nanoparticles were.

2.3.5 Measurement of zeta potential

We used the Malvern zeta seizer 2000 to find out the Zeta potential of AgNPs in water. Sonication was done for 5 minutes to make sure that the particles were spread out uniformly in the samples. Zeta potential analysis was used to find out the stability and surface potential of the AgNPs. The stability criteria of AgNPs were assessed when their zeta potential varied from above +30 mV to below −40 mV (Vijayakumar et al., 2013).

2.3.6 Energy Dispersive X-ray (EDX) Analysis Methodology

We used Energy Dispersive X-ray (EDX) spectroscopy linked to the SEM to find out what elements were in the nanoparticles. The same sample used for SEM imaging was tested to find and measure the elements present, which confirmed the composition and any capping or stabilizing chemicals that were present with the nanoparticles.

2.3.7 Scanning Electron Microscopy (SEM)

A Scanning Electron Microscope (SEM) was used to look at the shape and surface properties of the nanoparticles that were made. To improve electrical conductivity, the dried sample was put on a carbon-coated stub and covered with a thin layer of gold. We took pictures at several levels of magnification to see the shape, size, and surface features of the particles.

2.4. Antibacterial Activity

The manufactured nanoparticles' ability to kill bacteria was tested against four strains: Escherichia coli, Staphylococcus aureus, Bacillus subtilis, and Vibrio cholerae. We grew fresh bacterial cultures in nutrient broth and changed the turbidity to the usual level (0.5 McFarland). We did an agar well diffusion or disc diffusion experiment by evenly dispersing the bacterial suspension over nutrient agar plates. The nanoparticle solution was put into wells or discs, and the plates were kept at 37 °C for 24 hours. To test how well the antibiotic worked, we assessed the zone of inhibition around each well or disc. (Nguta, J. M., et al. 2019).

2.5 Activity of Antioxidants

2.5.1 DPPH Radical Scavenging Test:

The DPPH assay was used to find out how well *Pogostemon benghalensis* crude extract and AgNPs could get rid of free radicals. We made a 0.1 mM solution of DPPH in methanol and combined 1 mL of it with 1 mL of the test material at varied doses (10–200 µg/mL). The combination was left in the dark at room temperature for 30 minutes, and the absorbance was measured at 517 nm. We used ascorbic acid as a reference and figured out the IC_{50} values by figuring out the percentage of inhibition (Hussen et al., 2023).

2.5.2 Test for Scavenging Hydrogen Peroxide (H_2O_2)

To test hydrogen peroxide scavenging activity, a 40 mM H_2O_2 solution was made in phosphate buffer with a pH of 7.4. We mixed 1 mL of H_2O_2 solution to 1 mL of plant extract or nanoparticle suspension at different doses (10–200 µg/mL) and let it sit at room temperature for 10 minutes. Using phosphate buffer as a blank, we measured the drop in absorbance at 230 nm. Ascorbic acid served as the reference standard, and scavenging activity was quantified as the percentage inhibition of H_2O_2 (Pleh et al., 2021).

2.5.3 Phosphomolybdenum Antioxidant Test

The phosphomolybdenum technique (Prieto et al., 1999) was used to find the total antioxidant capacity. Three milliliters of reagent solution (0.6 M sulfuric acid, 28 mM sodium phosphate, and 4 mM ammonium molybdate) was added to 0.3 mL of extract or nanoparticle suspension. The combination was kept at 95 °C for 90 minutes in a water bath, then cooled to room temperature. The absorbance was measured at 695 nm. Ascorbic acid served as the standard, and antioxidant activity was quantified in ascorbic acid equivalents (mg AAE/g extract).

2.6. Test for cell viability

2.6.1. Induction of apoptosis: Anticancer tests (MTT, apoptosis)

We kept A549 (human lung adenocarcinoma) cells in DMEM with 10% FBS and 1% penicillin-streptomycin at 37 °C in a humidified 5% CO_2 incubator. To test for cytotoxicity, cells were placed in 96-well plates at a density of 1×10^4 cells per well and allowed to adhere for 18–24 hours. They were then treated with different amounts of *Pogostemon benghalensis* AgNPs (1–200 µg/mL) and appropriate controls (vehicle and positive control doxorubicin) for 24 and 48 hours in triplicate. After treatment, 20 µL of MTT reagent (5 mg/mL in PBS; final ~0.5 mg/mL) was applied per well and incubated for 3–4 hours at 37 °C. The formazan crystals were dissolved in 100 µL DMSO and the absorbance was determined at 570 nm (reference 630 nm). We used dose–response curves to figure out the cell viability (%) and IC_{50} values. To look at apoptosis, we collected treated and control cells from 6-well plates, washed them with cold PBS, and stained them with an Annexin V–FITC/PI apoptosis detection kit according to the manufacturer's instructions. We then used flow cytometry to look at the samples (collecting ≥10,000 events) and count the viable, early/late apoptotic, and necrotic populations. For the measurement of intracellular ROS, cells in 24-well plates were treated as previously described, incubated with 10 µM DCFH-DA in serum-free medium for 30 minutes at 37 °C in the dark, washed, and subsequently analyzed using flow cytometry (FITC channel) or a fluorescence microplate reader (Ex 485 nm / Em 530 nm); the data were presented as the fold-change in mean fluorescence intensity compared to the control. All studies were conducted in a minimum of three separate biological replicates, and the data were subjected to statistical analysis (ANOVA with post-hoc test), incorporating suitable biosafety and cell culture controls. (Maryam et al., 2017).

2.6.2 Analyzing Data

All studies were performed in triplicate, and the data were presented as mean ± standard deviation (SD). One-way analysis of variance (ANOVA) was used to find important differences between groups in the data. We used Tukey's HSD test for comparing more than one group or Dunnett's test for comparing against a control. When the assumptions of ANOVA were not satisfied, Welch's ANOVA or the Kruskal–Wallis test, succeeded by Dunn's post-hoc correction, was utilized. We used a four-parameter logistic regression model to make dose-response curves and get the half-maximal inhibitory concentration (IC_{50}). We used probit regression analysis to find the median lethal dose (LD_{50}). We used the right software (GraphPad Prism or R) for all of the statistical tests, and a p-value of less than 0.05 was considered statistically significant.

3. RESULT

3.1 Change in color during the synthesis of AgNPs

When you look at the three flasks side by side, you can see that the colors of the samples are different. Flask A has a yellowish-orange tint, which suggests that phytochemical activity is starting. Flask B looks practically colorless, which means that there is no reaction and it serves as the

control. Flask C is a rich brown color, which clearly shows that silver nanoparticles have formed. (Figure 1.)

3.2 Analysis of Vibrational Spectra (FTIR)

The FTIR spectra of the produced nanoparticles exhibited significant peaks associated with plant-derived functional groups. The 3279.12 cm^{-1} peak for O–H stretching showed that alcohols and phenols were present. The 2980.82 cm^{-1} band proved that CH_2/CH_3 groups were present. The signal at 1635.48 cm^{-1} indicated that there were either aromatic or unsaturated C=C groups. The existence of phenols, alcohols, and polyphenols involved in nanoparticle production was confirmed by further peaks at 1391.15, 1238.48, and 1068.08 cm^{-1}, which corresponded to O–H bending and C–O stretching (Table 1&2 and Figure 2&3). The FTIR spectra indicated a prominent O–H stretching band at 3372.43 cm^{-1}, which means that alcohols and phenolic chemicals are present. Peaks at 2949.93 cm^{-1} and 1405.98 cm^{-1} showed that CH_2/CH_3 was stretching and changing shape, which confirmed that alkanes were present. The 2838.75 cm^{-1} band was made up of O–H (acid) and C–H stretches that overlapped, which means that the compound is a carboxylic acid derivative. The 1635.88 cm^{-1} peak showed NH_2 scissoring of amines, while the 1018.94 cm^{-1} and 772.63 cm^{-1} peaks showed O–H bending in and out of the plane, which is what alcohols and phenols do.

3.3 UV–Vis Spectrum of Green-Synthesized AgNPs

The UV–Visible spectrum of the generated silver nanoparticles displayed a pronounced and sharp surface plasmon resonance peak at 440 nm, validating the effective synthesis of AgNPs. The plant extract alone, on the other hand, had a wide absorption band between 250 and 350 nm, which means that it had a lot of different phytochemical components. The appearance of a new peak at 440 nm alone in the nanoparticle sample shows that the bioactive chemicals in the *Pogostemon benghalensis* extract are able to turn silver ions into metallic silver. The lack of any extra peaks indicates that the nanoparticles that were made are stable, homogenous, and mostly monodispersed(Figure 4).

3.4 XRD pattern of AgNPs

The produced silver nanoparticles' XRD pattern has clear diffraction peaks at about $2\theta = 32°$, 38°, 46°, 64°, and 77°. These peaks correspond to the (111), (200), (220), and (311) crystallographic planes of face-centered cubic (FCC) silver. The (111) peak is the strongest of them, which means that this plane has a favored orientation and a lot of crystallinity. The crisp and well-defined peaks show that the nanoparticles are crystalline and don't have a lot of amorphous background. The lack of extra impurity peaks shows that the sample mostly has pure silver nanoparticles (Figure 5).

3.5 DLS Size Distribution of Nanoparticles

The Dynamic Light Scattering (DLS) test showed that the particles were all various sizes, with differential intensity going from 0 to 100 and cumulative intensity going from 1.0 to 1000.0. The nanoparticles had a z-average size of 113.6 nm, a polydispersity index (PDI) of 0.262, and a D(10)–D(90) range of 48.8–359.7 nm. These figures show that there are both small nanoparticles and bigger groups of particles in the colloidal suspension (Figure 6).

3.6 Zeta Potential of Nanoparticles

The zeta potential measurement reveals a distinct, pronounced peak situated near 0 mV, signifying that the produced nanoparticles have an extremely low surface charge. The tight distribution indicates consistent measurement values, and the peak location close to neutrality verifies the existence of weakly charged particles (Figure 7). The total counts over 400,000 indicate a robust signal intensity and reliable detection throughout the study.

3.7 SEM Microstructure of Synthesized Nanoparticles

The SEM micrograph taken at 25,000× magnification shows a lot of nanoparticles that are mostly spherical to almost spherical in shape. The particles look like bright, spherical shapes that come in different sizes, usually between 40 and 90 nm, with some bigger clusters of particles. The picture also shows areas of agglomeration, where nanoparticles have come together to form tight clusters. Smaller, individual nanoparticles are spread out around the edges (Figure 8).

3.8 EDX Study of Plant-Based AgNPs

The EDAX spectrum of the produced nanoparticles verified the existence of principal elemental constituents together with their respective weight and atomic percentages. Silver (Ag) had the highest weight percentage at 35.95%, which means that the nanoparticles were successfully formed. Carbon (C) and oxygen (O) were also present at 30.23% and 22.86%, respectively. These elements are usually found in plant-based organic compounds that stick to the surface of nanoparticles. There was a moderate quantity of chlorine (Cl) present, at 10.96%. This was probably due to the plant extract or the ingredients that were used to make it. The total elemental composition was 100%, which proved that the equipment was accurate and that the sample had the right amount of each element (Table 3&Figure:9).

3.9 Antibacterial Activity of Plant Extract

The plant extract's ability to kill bacteria was tested against four harmful kinds of bacteria: E. coli, S. aureus, B. subtilis and V. cholerae, with sample sizes of 25, 50, 75, and 100 µL. The findings indicated a dose-dependent augmentation in the zone of inhibition for all examined species. The inhibition zones were very small at the lowest concentration (25 µL), ranging from 0.38 ± 0.22 mm for E. coli to 1.80 ± 0.66 mm for V. cholerae. At 50 µL, there was

moderate suppression, although S. aureus (3.62 ± 0.24 mm) and V. cholerae (6.00 ± 0.20 mm) activity went up a lot. Higher doses (75–100 µL) resulted in significantly improved antibacterial effects, with peak inhibition observed at 100 µL. E. coli (7.40 ± 0.31 mm), S. aureus (9.76 ± 0.16 mm), B. subtilis (9.70 ± 0.34 mm) and V. cholerae (12.66 ± 0.30 mm). V. cholerae was the most sensitive strain to the extract, whereas E. coli was the least sensitive. Table 5 and Figure 10 reveal that E. coli had the weakest reaction (Table 4& Figure 10).

3.10. The Antioxidant Activity of Pb Silver Nanoparticles

Pogostemon benghalensis-mediated silver nanoparticles (PB AgNPs) shown dose-dependent antioxidant efficacy against DPPH, H_2O_2, and phosphomolybdenum radicals. At 100 µg, the inhibition was at its highest, with values of 81.49% (DPPH), 83.56% (H_2O_2), and 87.04% (phosphomolybdenum). The IC_{50} values were 60.69 µg (DPPH), 35.94–50 µg (H_2O_2), and 47.28–19.14 µg (phosphomolybdenum). This shows that table 4 has a lot of potential to get rid of free radical (Table 5).

3.11 Cytotoxicity and IC_{50} of AgPb NPs on A549 Cells

The anticancer assessment of AgPb nanoparticles against A549 lung cancer cells demonstrated a distinct dose-dependent enhancement in cytotoxicity. At lower concentrations (10–20 µg/mL), the nanoparticles caused a small drop in cell viability, with about 35–42% inhibition. The cytotoxic effect grew more significant as the dose increased, reaching about 60% inhibition at 100 µg/mL. The IC_{50} value we found was 47 µg/mL, which means that this amount is needed to kill 50% of A549 cells (Figure 11). In general, the results show that AgPb nanoparticles have strong antiproliferative effects on A549 cells.

4. DISCUSSION

The FTIR data show that a number of phytochemicals were actively involved in lowering and stabilizing the nanoparticles. The strong O–H peaks show that phenolic and alcoholic compounds work as natural reducing agents (Jothibas, et al., 2022). The C–H stretching at 2980.82 cm^{-1} shows that aliphatic groups like terpenoids help with capping and stabilization (Sidhu, et al., 2022). The 1635.48 cm^{-1} aromatic C=C peak shows that polyphenols give electrons to metal ions for reduction (Ponnusamy, et al., 2025). The other O–H and C–O peaks show that phenols, alcohols, and polysaccharides are present and are building a protective coating around the nanoparticles (Nagaraja, et al., 2023). The FTIR results show that different biomolecules were involved in the reduction and stability of the nanoparticles that were made. The pronounced O–H peaks signify the presence of phenolic and alcoholic chemicals functioning as natural reducing agents (Sreelekha et al., 2021; Vinoth et al.,2023; Gajendiran et al.,2025; Mohan et al.,2023). The aliphatic C–H vibrations indicate the existence of terpenoids and other hydrocarbon groups that facilitate nanoparticle capping (Khoee, et al., 2023; Sakthivel et al.,2026; Sandhiya et al.,2026; Manikandan et al.,2026). The carboxylic acid and amine-related peaks reveal supplementary functional groups that enhance nanoparticle surface binding and stabilization. The spectrum shows that polyphenols, alcohols, alkanes, and amino compounds all worked together to make nanoparticles (Meda et al.,2026[ab]; Mohan et al.,2026; Haq, et al., 2024).

The strong and well-defined surface plasmon resonance (SPR) peak at 440 nm provides clear evidence for the formation of spherical silver nanoparticles, as this wavelength is characteristic of collective electron oscillations on their surface (Rehman, et al., 2024)The shift from the broad absorption region of the plant extract (250–350 nm), which corresponds to phenolics, flavonoids, terpenoids, etc., to a sharp SPR band confirms that these phytochemicals played a significant role in reducing Ag^+ ions and stabilizing the resulting nanoparticles (Ritu, et al., 2023).The existence of a single, narrow SPR peak also indicates good optical stability, minimal agglomeration, and a uniform nanoscale particle distribution, because spherical, non-aggregated AgNPs typically show only one SPR band (Hamze, et al., 2025). These spectral characteristics collectively indicate that the green synthesis method successfully yielded stable and well-dispersed silver nanoparticles (Lasmi, et al., 2025).

The strong and well-defined diffraction peaks for the (111), (200), (220), and (311) planes show that the synthesized silver nanoparticles have a face-centered cubic (FCC) crystalline structure, which is the typical crystal shape for metallic silver (JCPDS No. 04-0783) (Sikdar, et al., 2023). The fact that the (111) plane has the most intensity means that the nanoparticles grow preferentially along this thermodynamically stable orientation, which is a trend that is often seen in green-synthesized AgNPs because plant-derived biomolecules affect nucleation and crystal growth (Albahri, et al., 2025). The sharpness and intensity of the peaks show that the crystals are very good quality, which means that Ag^+ ions were reduced quickly and nanoparticles were formed in a regulated way (Omran, et al., 2024). The lack of extra impurity peaks further supports the phase purity of the sample. This suggests that the phytochemicals in the extract not only acted as reducing agents but also as stabilizers, stopping oxidation or the formation of secondary phases (Atanassova, et al., 2025). Overall, the XRD pattern shows that the green synthesis method worked and made highly crystalline and phase-pure silver nanoparticles (Mannan, et al., 2024).

The DLS results show that the nanoparticles that were made are considerably polydisperse, as seen by the PDI value (0.262) and the wide D(10)–D(90) range. A PDI in

this range indicates a heterogeneous size distribution instead of a uniform (monodisperse) sample, a characteristic frequently noted in green-synthesized nanoparticles (Das et al., 2024; Palanisamy et al., 2025). The sharp increase in cumulative intensity suggests that bigger particles or groups of particles are blocking the light-scattering signal from smaller particles. This trend aligns with findings indicating that leftover biomolecules or insufficient reduction during green synthesis facilitate secondary aggregation (Cheng et al., 2021). The existence of bigger aggregates validates the successful creation of nanoparticles; nevertheless, it also underscores a deficiency in homogeneity. To precisely determine the actual core size and dispersion condition, it is imperative to employ complementary techniques such as transmission or scanning electron microscopy and zeta-potential measurements (Pei et al., 2025).

The zeta potential value near 0 mV shows that the nanoparticles that were made have low electrostatic stability. This is because nanoparticles with surface charges close to neutrality don't have enough repulsive forces to keep them from clumping together (Liu, et al., 2023). Low zeta potential values are common for green-synthesized nanoparticles, where plant-derived phytochemicals like polyphenols, flavonoids, and proteins stabilize particles by steric hindrance instead of electrostatic repulsion (Iskakova, et al., 2025). The abrupt, narrow peak in the distribution suggests that the nanoparticle population has a reasonably homogenous surface chemistry, although the proximity to 0 mV also signals an increased tendency for particle aggregation or clustering over time (Dghoughi, et al., 2025). The nanoparticles might stay stable in the near term because of organic capping layers, but to improve long-term colloidal stability, techniques like changing the pH or using stronger capping agents might be needed (Quinson, et al., 2023). The zeta potential profile corresponds with the standard characteristics of biologically produced nanoparticles, characterized by predominant steric stabilization and negligible electrostatic contributions (Fattahi et al., 2025).

The spherical or near-spherical shape we saw shows that the biosynthesis approach worked well to support the nanoparticles' uniform nucleation and development. The noticeable agglomeration is a common feature of green-synthesized nanoparticles, where plant-derived phytochemicals act as capping agents that primarily provide steric stabilization instead of strong electrostatic repulsion, resulting in partial clustering. The particle size range of ~40–90 nm is advantageous because nanosized spherical particles typically offer improved surface-area-to-volume ratios, enhancing their catalytic, antimicrobial, and biomedical performance (Singh, et al., 2023) The uniform brightness and smooth surface texture observed in the SEM micrograph further confirm successful nanoparticle formation; however, the presence of aggregates indicates that additional stabilization such as pH adjustment or stronger capping molecules may be necessary for improving dispersion stability and preventing long-term particle clustering (Spitzmüller, et al., 2024)

The EDAX profile clearly shows that silver nanoparticles were successfully made, as shown by the high silver weight percentage, which shows that Ag^{+} ions were effectively reduced to metallic Ag^{0} during synthesis (Naveed, et al., 2024). The presence of carbon and oxygen shows that plant-derived phytochemicals like flavonoids, phenolics, proteins, and other organic compounds were involved. These biomolecules stick to the nanoparticle surface, forming a stabilizing organic layer that keeps the nanoparticles from clumping together and improves colloidal stability. The small chlorine signal could come from natural parts of the plant extract or leftover salts from the reaction medium, which is something that happens a lot when making nanoparticles with phytochemicals (Sadiq, et al., 2023). The elemental distribution strongly supports a green synthesis mechanism and shows that the nanoparticles are mostly made of silver with a surface rich in phytochemicals that gives them their stability and functional properties (Arthi, et al., 2025).

The antibacterial test showed a clear dose-dependent response, which means that larger amounts of the extract have enough bioactive chemicals to stop bacterial cell activities. The relatively low inhibition zones at 25 and 50 µL indicate that the concentrations of phytochemicals at these levels were inadequate for significant bactericidal effects, corroborating previous research that demonstrates plant-derived metabolites exhibit enhanced activity solely at elevated doses (Challa et al., 2025). The heightened inhibition noted at 75 and 100 µL may result from elevated levels of phenolics, flavonoids, and terpenoids, which are recognized for disrupting membrane integrity, protein functionality, and DNA replication (Velmani, et al., 2025). V. cholerae's higher susceptibility may be due to its weaker peptidoglycan structure, which makes it easier for phytochemicals to get through. E. coli exhibited decreased inhibition, aligning with findings indicating Gram-negative bacteria have outer membrane barriers that impede phytochemical absorption (Said et al., 2025; Khajuria et al., 2025). Overall, the results show that the plant extract has a lot of antibacterial activity, especially at higher doses (El-Saadony, et al., 2025).

Pogostemon benghalensis-mediated silver nanoparticles (PB AgNPs) exhibited strong, concentration-dependent antioxidant activity in DPPH, H_2O_2, and phosphomolybdenum tests, with inhibition escalating from 15–59% at 20–80 µg to 81–87% at 100 µg. The IC_{50} values (DPPH: 60.69 µg, H_2O_2: 35.94–50 µg,

phosphomolybdenum: 19.14–47.28 µg) show that these substances have a moderate to strong ability to scavenge radicals (Hussen, et al., 2023). This activity is due to phytochemicals like phenolics and flavonoids on the surface of the nanoparticles. These chemicals give electrons to free radicals to neutralize them. This is a common way that plant-mediated AgNPs work (Ritu, et al., 2023). Similar antioxidant effects have been seen in AgNPs made from other medicinal plants, which shows that green synthesis can be used to make bioactive nanoparticles (Hanachi, et al., 2022). Overall, PB AgNPs show good promise as antioxidants in vitro, but their activity may be a little lower than that of typical antioxidants since some of their active functional groups are capped.

The anticancer activity of AgPb nanoparticles against A549 lung cancer cells exhibited a distinct dose-dependent inhibitory effect, resulting in an IC_{50} value of 47 µg/mL, consistent with the moderate cytotoxic potency typically associated with green-synthesized silver nanoparticles (Pandey et al., 2025). The gradual rise in growth inhibition from 10 to 100 µg/mL suggests effective cellular absorption and interaction of AgNPs with intracellular components, ultimately disrupting metabolic processes and proliferation (Barua et al., 2024). Previous research has demonstrated that AgNPs provoke the formation of reactive oxygen species (ROS), mitochondrial membrane depolarization, and death in A549 cells, indicating the potential for AgPb nanoparticles to operate via analogous pathways (Li et al., 2021). Biosynthesized AgNPs are known to activate mitochondrial-mediated apoptotic pathways by altering p53, Bax, Bcl-2, and caspase signaling, which may elucidate the observed cytotoxicity (Pathan, et al., 2025). The minor plateau in inhibition at elevated concentrations indicates saturation of cellular contact sites or the peak capacity for ROS generation (Zhuang et al., 2024). Overall, the findings demonstrate that AgPb nanoparticles have considerable anticancer efficacy against A549 cells via oxidative stress-mediated and mitochondria-driven apoptotic pathways.

The AO/EtBr dual-staining results unequivocally illustrate that AgPb nanoparticles elicit apoptosis in A549 lung cancer cells in a dose-dependent fashion. The treated groups exhibited a significant transition from uniformly green, viable cells to heterogeneous populations of yellow, orange, and brightly red cells, signifying both early and late apoptosis, along with a compromise in membrane integrity. This transition indicates that AgPb nanoparticles induce cytotoxicity predominantly via apoptotic pathways rather than necrotic damage (Thirumurugan et al.,2026; Karthikeyan et al.,2025;Ayyadurai et al.,2026; Mohamed et al., 2022). The morphological alterations noted, including chromatin condensation, nuclear fragmentation, and decreased cell density, are definitive signs of nanoparticle-induced oxidative stress and mitochondrial dysfunction, frequently documented in biosynthesized silver nanoparticles (Chandramohan et al., 2024; Hellany et al., 2025). The significant rise in apoptotic cells in the treated samples corresponds with the IC_{50} value reported in the cytotoxicity assay, corroborating the robust antiproliferative efficacy of AgPb nanoparticles against lung cancer cells. The staining results demonstrate that AgPb nanoparticles efficiently disturb cellular homeostasis and start programmed cell death, underscoring their potential as a biologically active anticancer treatment (Muhamad et al., 2022).

Table: 1 FTIR of *Pogostemon benghalensis* – functional groups before the production of silver nanoparticles

S.No	Peak value	Molecular mention	Vibration intensity	Functional group
1	3279.12	O-H (H-bonded)	Stretch/str	Alcohols & Phenols
2	2980.82	CH_3,CH_2,CH2 or 3 bands	Stretch/str	Alkanes
3	1635.48	C=C(symmetry reduces intensity)	Bend/med	Alkanes
4	1391.15	O-H bending (in-plane)	Bend/med	Alcohols & Phenols
5	1238.48	O-H bending (in-plane)	Stretch/str	Alcohols & Phenols
6	1068.08	O-H bending	Stretch/str	Alcohols & phenols

Table 2: FTIR of silver nanoparticles produced by *Pogostemon benghalensis*, displaying typical functional groups.

S.no	Peak value	Molecular mention	Vibration indensity	Functional group
1	3372.43	O-H (H-bonded)	Stretch/str	Alcohols & Phenol
2	2949.93	CH_2, CH_3 & CH 2 or 3 bands	Stretch/str	Alkanes
3	2838.75	O-H (acid) overlap C-H	Stretch/var	Carboxylic acid & Derivatives
4	1635.88	NH_2 Scissoring (1^0-amines)	Bend/med	Amines
5	1405.98	CH_2 & CH_3 deformation	Bend/med	Alkanes
6	1018.94	O-H bending (in-plane)	Stretch/str	Alcohols & Phenol
7	772.63	O-H bending (out -of- plane)	Bend/wk	Alcohols & Phenol

Table:3 EDX spectrum of silver nanoparticles made using *Pogostemon benghalensis*.

Lineee	Weight %	Weight % Error	Atom %
C K	30.23	± 1.28	54.85
O K	22.86	± 1.34	31.14
Cl K	10.96	± 0.56	6.74
Cl L	---	---	---
Ag L	35.95	± 2.33	7.26
Ag M	---	---	---
Total	100.00		100.00

Table 4: *The antioxidant activity of the synthesized silver nanoparticles extract from Pogostemon benghalensis leaves was assessed using DPPH, H_2O_2, and phosphomolybdenum assays.*

Concentration µg	Inhibitation (%)					
	DPPH		H2O2		Phosphomolebidinam	
	PB AgNps	AA	PB AgNps	AA	PB AgNps	AA
20	15.74±0.67	50.17±0.65	8.733±0.09	1.60±0.41	33.72±0.59	46.57±0.28
40	30.29±0.34	55.94±0.94	19.61±0.56	14.23±0.58	42.32±0.42	59.97±0.49
60	48.54±3.82	82.84±0.58	43.72±0.58	32.09±0.80	54.48±0.08	82.84±0.58
80	59.92±0.49	84.86±0.25	67.11±0.060	43.63±0.71	76.56±0.06	86.50±0.05

100	81.49±0.32	88.55±0.01	83.56±0.083	59.89±0.58	87.04±0.03	90.13±0.07
IC50 Value	**60.69**	**17.48**	**35.94**	**50**	**47.28**	**19.14**

PB AgNps = Silver Nanoparticles of Pogostemon benghalensis; **AA =** Ascorbic Acid

Table 5: Antibacterial Activity of Synthesized Silver Nanoparticles Against Pathogenic Bacteria

S.No	Strains	Sample	Zone of inhibition (mm)				
			25 µL	**50 µL**	**75 µL**	**100 µL**	**Control 10 µL**
1	***E. coli***	**AgNPs**	0.38±0.22	1.30±0.50	4.32 ±0.42	7.40±0.31	11.66±1.33
2	***S. aureus***		1.11±0.12	3.62±0.24	5.423±0.45	9.76±0.16	14.2±0.16
3	***B. subtilis***		0.40±0.22	1.22±0.43	6.32±0.71	9.70±0.34	13.53±0.24
4	***V. cholerae***		1.80±0.66	6.00±0.20	8.06±0.22	12.66±0.3	15.16±0.33

AgNPs = Silver Nanoparticles; **E. coli -** Escherichia coli, **S. aureus -** Staphylococcus aureus, **B. subtilis -** Bacillus subtilis and **V. cholerae -** Vibrio cholerae

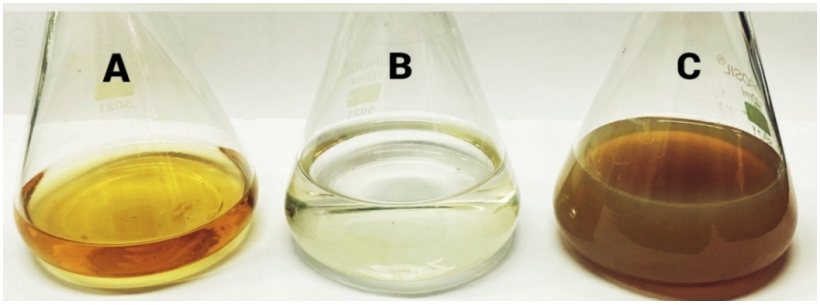

Figure:1. Color Change During the Making of Silver Nanoparticles

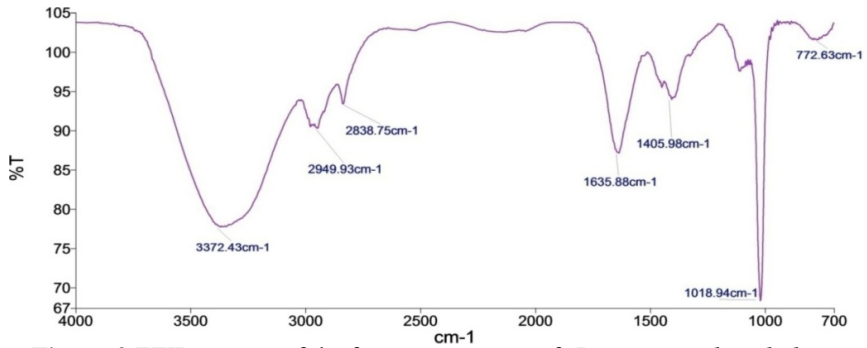

Figure:2 FTIR spectra of leaf aqueous extract of *Pogostemon benghalensis*

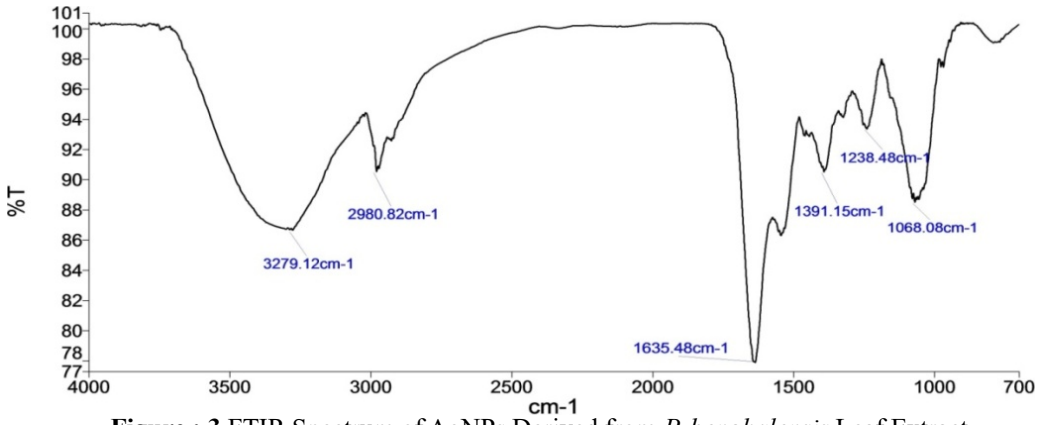

Figure : 3 FTIR Spectrum of AgNPs Derived from *P. benghalensis* Leaf Extract

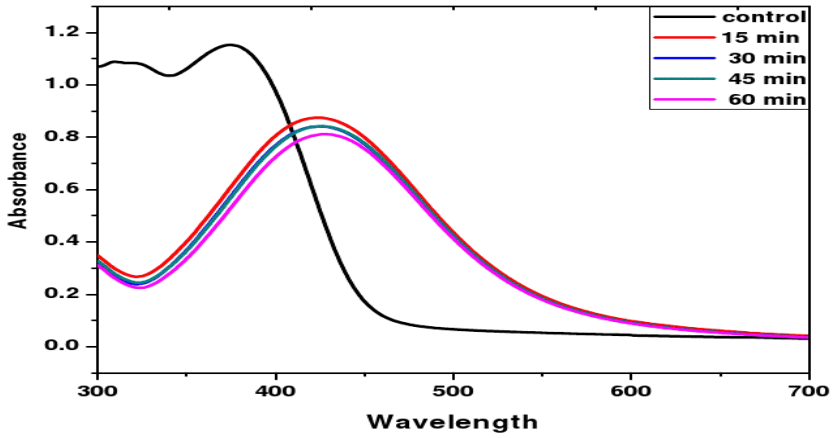

Figure: 4 UV Spectrum of *P. benghalensis*–Mediated AgNPs

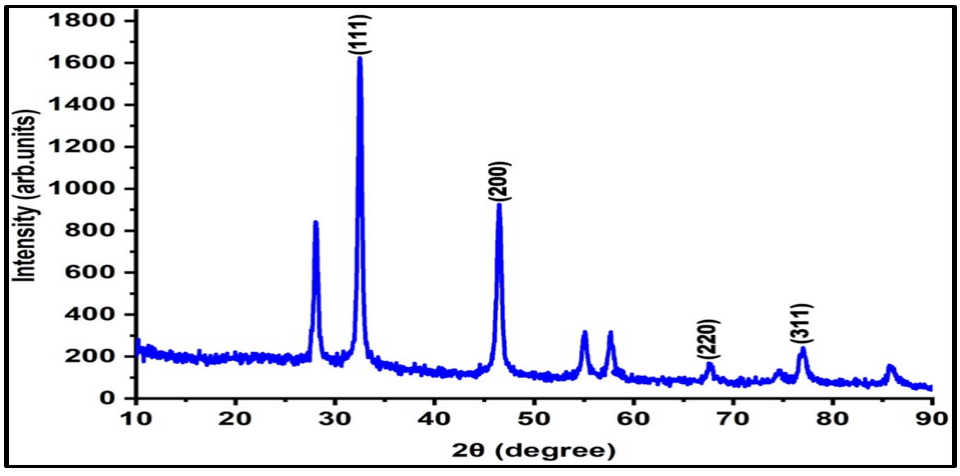

Figure: 5 XRD Spectrum of AgNPs Mediated by P. benghalensis

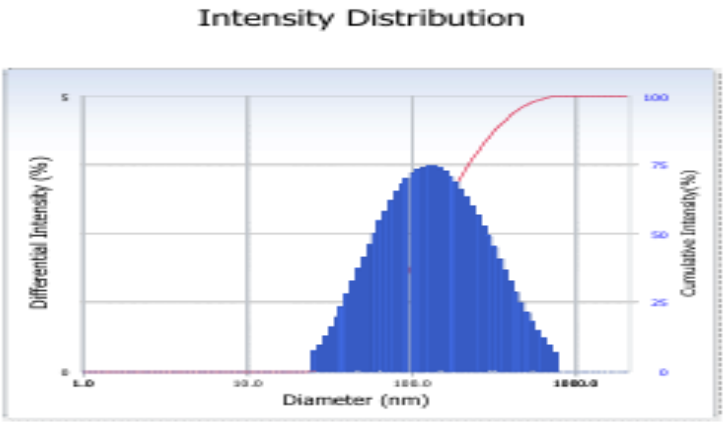

Figure : 6 The DLS Intensity Distribution Curve

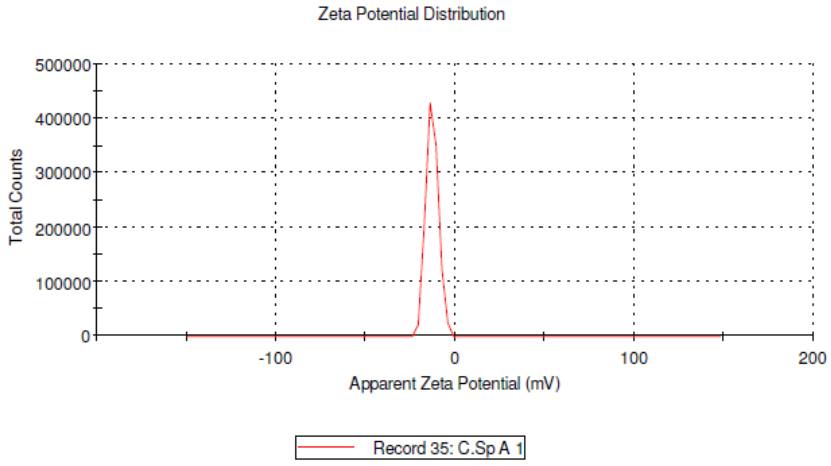

Figure :7 Zeta Potential of *P. benghalensis*–Mediated AgNPs

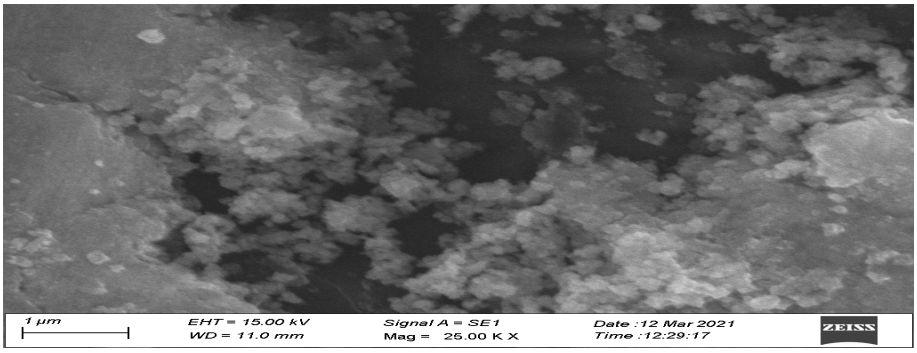

Figure : 8 SEM image of silver nanoparticles that were made with *Pogostemon benghalensis***.**

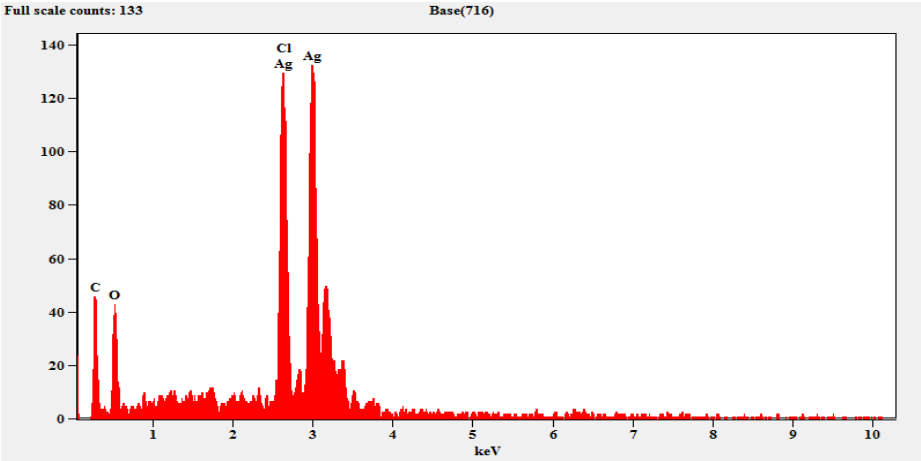

Figure :9 shows the EDX spectrum of silver nanoparticles that *Pogostemon benghalensis* has made.

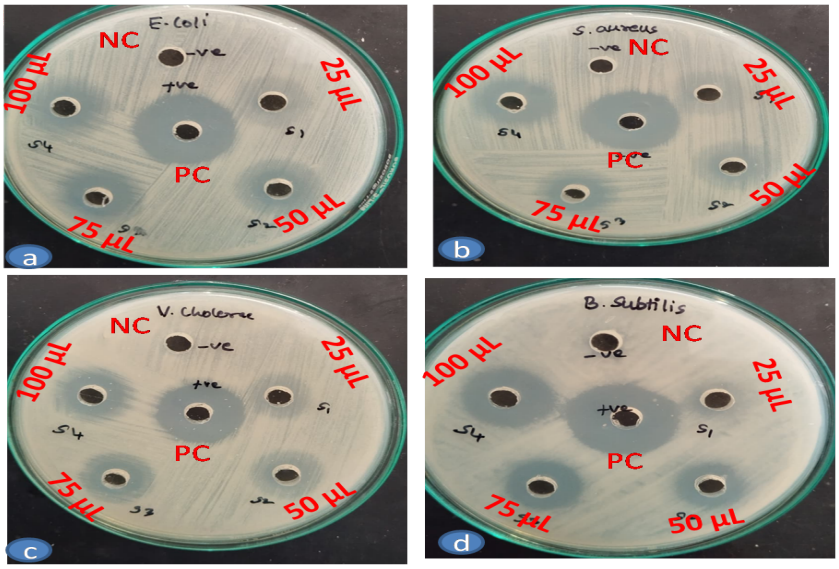

Figure:10 The antibacterial properties of *Pogostemon benghalensis* silver nanoparticles against E. coli, S. aureus, V. cholerae, and B. subtilis**.**

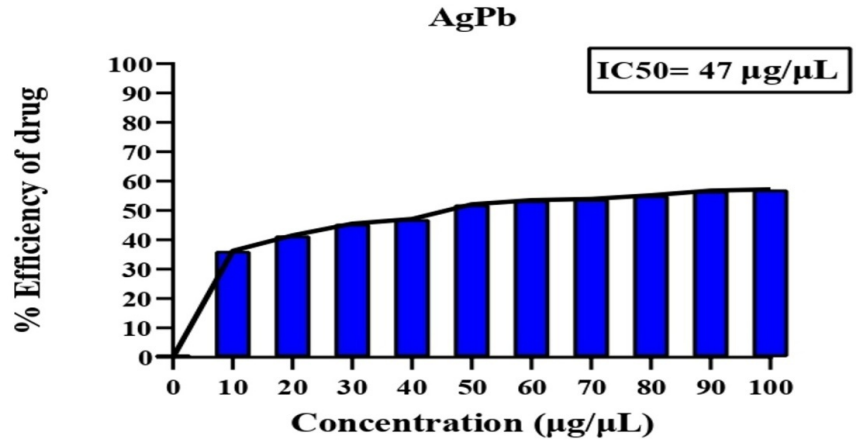

Figure :11 shows how the cytotoxicity of AgPb nanoparticles depends on their concentration and affects cell viability.

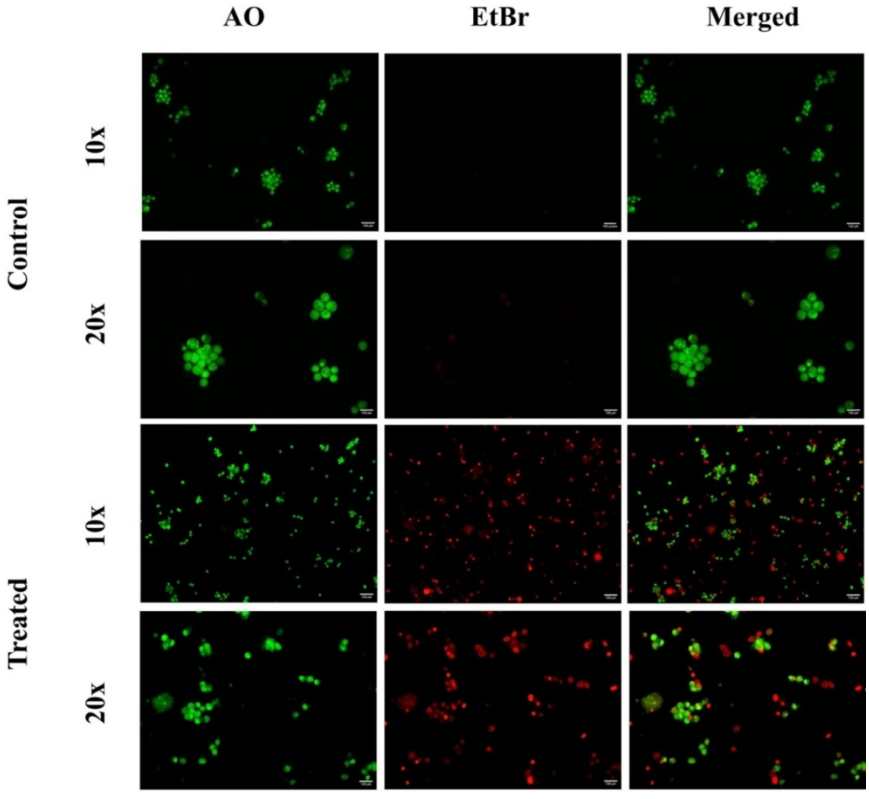

Figure : 12 AO/EtBr staining shows that both control and AgPb-treated cells are dying.

CONCLUSION

The work effectively proved the eco-friendly synthesis of silver nanoparticles using *Pogostemon benghalensis* extract, confirmed through visual observation, spectral analysis, crystalline structure validation, and morphological characterisation. FTIR identified functional groups that were very important in decreasing and stabilizing the nanoparticles. The UV–Vis and XRD data demonstrated that stable, crystalline AgNPs had formed. The SEM and DLS results showed that the particles were polydispersed spheres that were somewhat aggregated. The biosynthesized AgNPs demonstrated substantial antibacterial efficacy against both Gram-positive and Gram-negative pathogens, pronounced antioxidant properties, and significant cytotoxicity against A549 lung cancer cells. The induction of apoptosis was convincingly established using AO/EtBr staining, indicating that the nanoparticles promote programmed cell

death. Thus, *Pogostemon benghalensis* produced AgNPs constitute a potent, natural, and environmentally sustainable platform with prospective applications in nanomedicine, antibacterial formulations, and anticancer therapy.

Authors' contributions
TM: Conceptualization, Methodology, Investigation, Writing - original draft, Writing - Review & Editing, Validation, Formal analysis. AT, SV & KV Conceptualization, Writing - Review & Editing, Validation, Formal analysis. AL: Formal analysis, Data curation, Software, Resources, Validation.

Funding
The authors declare that this study has no funding

Statements and Declarations

Declaration of competing interest

The authors declare that there is no conflict of interest.

Data availability
All data supporting this research will be made available on request.

Ethical approval
Not applicable.

REFERENCE

1) Adetunji, T. L., Olisah, C., Acho, M. A., Oyetunde-Joshua, F., & Amoo, S. O. (2024). Global research trends and recent advances in medicinal plant-synthesized nanoparticles for cancer treatment. Plants, 13(20), 2836.

2) Albahri, G., Badran, A., Hellany, H., Kafrouny, N., El Kurdi, R., Alame, M., ... & Baydoun, E. (2025). Green Synthesis of Gold Nanoparticles Using Mandragora autumnalis: Characterization and Evaluation of Its Antioxidant and Anticancer Bioactivities. Pharmaceuticals, 18(9), 1294.

3) Arthi, P., Hema, K., Rani, S. V. G., Sugarthi, R., Sivapunniyam, A., Perumal, T., ... & Jayashree, C. (2025). Myco-Engineered Magnesium Oxide (MgO) Nanoparticles from Ayapana triplinervis Endophyte: A Dual-Functional Approach for Biomedical and Environmental Applications. Journal of Inorganic and Organometallic Polymers and Materials, 1-20.

4) Atanassova, M., Zahnit, W., Messaoudi, M., Rebiai, A., Benchikha, N., & Sawicka, B. (2025). Analytical Techniques for Phytochemical Analysis and Functional Investigation. In Biotechnology and Phytochemical Prospects in Drug Discovery (pp. 151-187). Singapore: Springer Nature Singapore.

5) Ayyadurai, T., Mohan, P. K., Annamalai, A., Kamaraj, C., & Waheeb, M. Q. (2026). Biogenic silver nanoparticles synthesis from Guilandina bonduc L. seed kernel extract with antibacterial, antioxidant and anticancer potential against ovarian Cancer cells. Results in Chemistry, 103246.

6) Ayyadurai, T., Moola, A.K., Mohan, P.K., Thiruppathi, S.K., Shanmugam, A. and Bollipo Diana, R.K., 2022. Ameliorative effects of Guilandina bonduc L. aqueous seed extract on letrozole induced polycystic ovary syndrome in female wistar albino rats. Advances in Traditional Medicine, 22(4), pp.885-903.

7) Balata, H., Fong, K. M., Hendriks, L. E., Lam, S., Ostroff, J. S., Peled, N., ... & Aggarwal, C. (2019). Prevention and early detection for NSCLC: advances in thoracic oncology 2018. Journal of Thoracic Oncology, 14(9), 1513-1527.

8) Barathi, S., Ramalingam, S., Krishnasamy, G., & Lee, J. (2024). Exploring the biomedical frontiers of plant-derived nanoparticles: Synthesis and biological reactions. Pharmaceutics, 16(7), 923.

9) Barua, N., & Buragohain, A. K. (2024). Therapeutic potential of silver nanoparticles (agnps) as an antimycobacterial agent: a comprehensive review. Antibiotics, 13(11), 1106.

10) Begum, S. J., Pratibha, S., Rawat, J. M., Venugopal, D., Sahu, P., Gowda, A., ... & Jaremko, M. (2022). Recent advances in green synthesis, characterization, and applications of bioactive metallic nanoparticles. Pharmaceuticals, 15(4), 455.

11) Bertolaccini, L., Casiraghi, M., Uslenghi, C., Maiorca, S., & Spaggiari, L. (2024). Recent advances in lung cancer research: unravelling the future of treatment. Updates in Surgery, 76(6), 2129-2140.

12) Challa, B. R., Kantamneni, G. D., Suravajhala, M., Vadlamudi, S., Manne, M., & Chathyushya, K. B. (2025). Phytochemical analysis and bioactive potential of Moringa, Eucalyptus, and Nerium extracts against microbial, diabetic, inflammatory, and oxidative stress challenges. 3 Biotech, 15(11), 401.

13) Chandraker, S. K., & Kumar, R. (2024). Biogenic biocompatible silver nanoparticles: a promising antibacterial agent. Biotechnology and Genetic Engineering Reviews, 40(4), 3113-3147.

14) Chandramohan, S., Francis, A. P., Pajaniradje, S., & Rajagopalan, R. (2024). Green and chemical synthesized zinc oxide nanoparticles: Evaluation of their anti-proliferative activity against breast cancer cell line–An in vitro and in silico approach. Particulate Science and Technology, 42(7), 1155-1177.

15) Cheng, Y., Saggu, M., & Thomas, J. C. (2021). Analysis of Aggregates and Particles. In Protein Instability

at Interfaces During Drug Product Development: Fundamental Understanding,

16) Chowdhury synthesis and their diverse applications. In Ethnopharmacology and OMICS Advances in Medicinal Plants Volume 2: Revealing the Secrets of Medicinal Plants (pp. 213-250). Singapore: Springer Nature Singapore.

17) Dahiya, S., Batish, D. R., & Singh, H. P. (2020). Ethnobotanical, phytochemical and pharmacological aspects of Bengal Pogostemon (*Pogostemon benghalensis*). Journal of Herbmed Pharmacology, 9(4), 318-327.

18) Das, M. R., Hussain, N., Duarah, R., Sharma, N., Sarmah, P., Thakur, A., ... & Boukherroub, R. (2024). Metal nanoparticles decorated two-dimensional nanosheets as heterogeneous catalysts for coupling reactions. Catalysis Reviews, 66(3), 923-995.

19) Dghoughi, A., Raji, M., Chakchak, H., Bensalah, M. O., Bouhfid, R., & Qaiss, A. E. K. (2025). Synthesis of triangular lignin photonic crystal nanoparticles: Investigating solvent effects and dialysis optimization. International Journal of Biological Macromolecules, 291, 139110.

20) Eker, F., Akdaşçi, E., Duman, H., Bechelany, M., & Karav, S. (2025). Green synthesis of silver nanoparticles using plant extracts: A comprehensive review of physicochemical properties and multifunctional applications. International Journal of Molecular Sciences, 26(13), 6222.

21) El-Saadony, M. T., Saad, A. M., Mohammed, D. M., Korma, S. A., Alshahrani, M. Y., Ahmed, A. E., ... & Ibrahim, S. A. (2025). Medicinal plants: bioactive compounds, biological activities, combating multidrug-resistant microorganisms, and human health benefits-a comprehensive review. Frontiers in immunology, 16, 1491777.

22) Fattahi, N., Khan, F., Kim, N. G., Tabassum, N., Kim, T. H., Kim, Y. M., & Jung, W. K. (2025). Investigation of lignin content in the fabrication of ZnO NPs and their antioxidant, antibiofilm, and antimicrobial properties. BioNanoScience, 15(1), 19..

23) Gajendiran, J., Sawyasasin, D., Udhayachozhan, P., Gnanam, S., Ramya, J. R., Balraju, P., ... & Sabarish, V. B. (2025). Synthesis and physico-chemical characterization of ZnO nanostructures for LED, photocatalytic, and biomedical applications. Journal of the Indian Chemical Society, 102(8), 101867.

24) González-Vega, J. G., García-Ramos, J. C., Chavez-Santoscoy, R. A., Castillo-Quiñones, J. E., Arellano-Garcia, M. E., & Toledano-Magaña, Y. (2022). Lung models to evaluate silver nanoparticles' toxicity and their impact on human health. Nanomaterials, 12(13), 2316.

25) Grewal, J., Kumar, V., Rawat, H., Gandhi, Y., Singh, R., Singh, A., ... & Mishra, S. K. (2022). Cytotoxic effect of plant extract-based nanoparticles on cancerous cells: a review. Environmental Chemistry Letters, 20(4), 2487-2507.

26) Hamze, Z. K., Assi, S., Mhanna, R., Bouaziz, M., Said, M. E. A., Benouis, K., ... & El-Dakdouki, M. H. (2025). Sustainable preparation of multifunctional green silver nanoparticles for efficient catalytic dye degradation and bacterial inhibition. Environmental Science and Pollution Research, 32(39), 22698-22718.

27) Hanachi, P., Gharari, Z., Sadeghinia, H., & Walker, T. R. (2022). Synthesis of bioactive silver nanoparticles with eco-friendly processes using Heracleum persicum stem extract and evaluation of their antioxidant, antibacterial, anticancer and apoptotic potential. Journal of Molecular Structure, 1265, 133325.

28) Haq, S. I. U., Wali, S., Sama, N. U., Kamran, K., Ullah, Z., & Mohamed, H. I. (2024). Environmentally friendly synthesis of silver nanoparticles (AgNPs) using Mentha arvensis plants modulates physiological and biochemical attributes and yield of sunflower (Helianthus annuus L.). Journal of Soil Science and Plant Nutrition, 24(2), 3610-3630.

29) Hellany, H., Badran, A., Albahri, G., Kafrouny, N., El Kurdi, R., Maresca, M., ... & Baydoun, E. (2025). Biogenic Synthesis of Gold Nanoparticles Using Scabiosa palaestina Extract: Characterization, Anticancer and Antioxidant Activities. Nanomaterials, 15(17), 1368.

30) Hosny, S., Gaber, G. A., Ragab, M. S., Ragheb, M. A., Anter, M., & Mohamed, L. Z. (2025). A Comprehensive Review of Silver Nanoparticles (AgNPs): Synthesis Strategies, Toxicity Concerns, Biomedical Applications, AI-Driven Advancements, Challenges, and Future Perspectives. Arabian Journal for Science and Engineering, 1-48.

31) Hussen, E. M., & Endalew, S. A. (2023). In vitro antioxidant and free-radical scavenging activities of polar leaf extracts of Vernonia amygdalina. BMC complementary medicine and therapies, 23(1), 146.

32) Ibrahim, B., & Ezeorba, T. P. C. (2025). Global research trends on gold and silver nanoparticle-induced cytotoxicity in cancer cells: a bibliometric perspective. Results in Engineering, 106379.

33) Iskakova, Z., Kozhantayeva, A., Temirbekova, A., Mukhtubayeva, S., Bissenova, G., Tekebayeva, Z., ... & Sarmurzina, Z. (2025). Green Synthesis of Silver Nanoparticles Using Circaea lutetiana EthanolicExtract:

Phytochemical Profiling, Characterization, and Antimicrobial Evaluation. International Journal of Molecular Sciences, 26(12), 5505.

34) Jain, N., Jain, P., Rajput, D., & Patil, U. K. (2021). Green synthesized plant-based silver nanoparticles: Therapeutic prospective for anticancer and antiviral activity. Micro and Nano Systems Letters, 9(1), 5.

35) Jaishwal, N., Jayswal, M., Gupta, D. C., Dhakal, B., Koirala, S., Khadka, R. B., ... & Pandey, J. (2025). Bioactive Potential of *Pogostemon benghalensis* (Burm. f.) Kuntze: Antibacterial, Antioxidant, and Xanthine Oxidase Inhibitory Activities. Bacteria, 4(1), 3.

36) Jeyaram, M., Jeyaram, Y., Ayyadurai, T., Gurusamy, M. (2026). Exploration of Streptomycetes as Biocontrol Agents Against Plant Pathogens. In: Kaur, T., Kumar, H., Manhas, R.K. (eds) Streptomycetes: Biological Candidates for Sustainable Agriculture. Springer, Singapore. https://doi.org/10.1007/978-981-95-5803-2_6

37) Jothibas, M., Paulson, E., Srinivasan, S., & Kumar, B. A. (2022). The impacts of interfacing phytochemicals on the structural, optical and morphology of hematite nanoparticles. Surfaces and Interfaces, 29, 101734.

38) Karthikeyan, M., Gajendiran, J., Gnanam, S., Ramya, J.R., Arul, K.T., Khedulkar, A.P., Siddheswaran, R., Synthesis of undoped and mixed binary transition metals (Ni-co)- doped cupric oxide nanostructures: structural characteristics, optical behavior, and biological activity, J. Mol. Struct. 1321 (2025) 139895.

39) Khajuria, A. K., Kandwal, A., Sharma, R. K., Bachheti, R. K., Worku, L. A., & Bachheti, A. (2025). In vitro antioxidant and antibacterial activities of biogenic synthesized zinc oxide nanoparticles using leaf extract of Mallotus philippinensis Mull. Arg. Scientific Reports, 15(1), 6541.

40) Khoee, S., & Madadi, M. (2023). Medicinal plant-based terpenoids in nanoparticles synthesis, characterization, and their applications. In Secondary Metabolites from Medicinal Plants (pp. 53-86). CRC Press.

41) Kulkarni, D., Sherkar, R., Shirsathe, C., Sonwane, R., Varpe, N., Shelke, S., ... & Dyawanapelly, S. (2023). Biofabrication of nanoparticles: sources, synthesis, and biomedical applications. Frontiers in bioengineering and biotechnology, 11, 1159193.

42) Kumar, A., Sharma, N., Chanotiya, C. S., & Lal, R. K. (2024). The pharmacological potential and the agricultural significance of the aromatic crop Patchouli (Pogostemon cablin Benth.): A review. Ecological Frontiers, 44(6), 1109-1118.

43) Kumara Swamy, M., Sudipta, K. M., Jayanta, K., & Balasubramanya, S. (2015). The green synthesis, characterization, and evaluation of the biological activities of silver nanoparticles synthesized from Leptadenia reticulata leaf extract. Applied nanoscience, 5(1), 73-81.

44) Lasmi, F., Hamitouche, H., Laribi-Habchi, H., Benguerba, Y., & Chafai, N. (2025). Silver Nanoparticles (AgNPs), Methods of Synthesis, Characterization, and Their Application: A Review. Plasmonics, 1-34.

45) Leiter, A., Veluswamy, R. R., & Wisnivesky, J. P. (2023). The global burden of lung cancer: current status and future trends. Nature reviews Clinical oncology, 20(9), 624-639.

46) Li, L., Bi, Z., Hu, Y., Sun, L., Song, Y., Chen, S., ... & Wei, X. (2021). Silver nanoparticles and silver ions cause inflammatory response through induction of cell necrosis and the release of mitochondria in vivo and in vitro. Cell biology and toxicology, 37(2), 177-191.

47) Liu, Y. L., Li, Y., Si, Y. F., Fu, J., Dong, H., Sun, S. S., ... & Zhang, Z. Q. (2023). Synthesis of nanosilver particles mediated by microbial surfactants and its enhancement of crude oil recovery. Energy, 272, 127123.

48) Mannan, M. A., Rubel, M. H. K., Rahman, M. A., Hamid, A. U., Uddin, M. B., Kitamura, S., ... & Kida, T. (2024). Solvothermal synthesis, crystal structure, multifunctioning characterizations and anti-microbial activity assessment of Ag doped h-BN through silver diethyldithiocarbamate. Journal of Alloys and Compounds, 1002, 175139.

49) Maryam, A., Mehmood, T., Zhang, H., Li, Y., Khan, M., & Ma, T. (2017). Alantolactone induces apoptosis, promotes STAT3 glutathionylation and enhances chemosensitivity of A549 lung adenocarcinoma cells to doxorubicin via oxidative stress. Scientific reports, 7(1), 6242.

50) Mehta, K., Maass, C., Cucurull-Sanchez, L., Pichardo-Almarza, C., Subramanian, K., Androulakis, I. P., ... & Sherwin, C. M. (2025). Modernizing Preclinical Drug Development: The Role of New Approach Methodologies. ACS Pharmacology & Translational Science.

51) Mohamed, A. F., Nasr, M., Amer, M. E., Abuamara, T. M., Abd-Elhay, W. M., Kaabo, H. F., ... & Shebl, R. I. (2022). Anticancer and antibacterial potentials induced post short-term exposure to electromagnetic field and silver nanoparticles and related pathological and genetic alterations: in vitro study. Infectious Agents and Cancer, 17(1), 4.

52) Mohan, P.K., Krishna, T.A., Stephy, P.P., Thirumurugan, A., Kumar, T.S. and Kumari, B.R., 2023. Nano-engineered silver rods from Pleurolobus gangeticus

root extract and their antilithiatic and cytoprotective role on oxalate injured renal epithelial cells. Biocatalysis and Agricultural Biotechnology, 52, p.102837.

53) Muhamad, M., Ab. Rahim, N., Wan Omar, W. A., & Nik Mohamed Kamal, N. N. S. (2022). Cytotoxicity and Genotoxicity of Biogenic Silver Nanoparticles in A549 and BEAS-2B Cell Lines. Bioinorganic Chemistry and Applications, 2022(1), 8546079.

54) Muthukrishnan, S., Bhakya, S., & Ramalingam, V. (2025). Metal nanoparticles synthesis: an overview of different synthesis methods, mode of action and their biomedical application. Discover Applied Sciences, 7(10), 1079.

55) Nagaraja, K., Hemalatha, D., Ansar, S., & Hwan, O. T. (2023). Novel, biosynthesis of palladium nanoparticles using strychnos potatorum polysaccharide as a green sustainable approach; and their effective catalytic hydrogenation of 4-nitrophenol. International Journal of Biological Macromolecules, 253, 126983.

56) Narayanan, M., Divya, S., Natarajan, D., Senthil-Nathan, S., Kandasamy, S., Chinnathambi, A., ... & Pugazhendhi, A. (2021). Green synthesis of silver nanoparticles from aqueous extract of Ctenolepis garcini L. and assess their possible biological applications. Process Biochemistry, 107, 91-99.

57) Naveed, M., Mahmood, S., Aziz, T., Azeem, A., Rajpoot, Z., Rehman, S. U., ... & Alshareef, S. A. (2024). Green-synthesis of silver nanoparticles AgNPs from Podocarpus macrophyllus for targeting GBM and LGG brain cancers via NOTCH2 gene interactions. Scientific Reports, 14(1), 25489.

58) Ng, C. X., Affendi, M. M., Chong, P. P., & Lee, S. H. (2022). The potential of plant-derived extracts and compounds to augment anticancer effects of chemotherapeutic drugs. Nutrition and Cancer, 74(9), 3058-3076.

59) Nguta, J. M., et al. (2019). Phytochemical composition and antimicrobial activity of crude extracts from Kenyan medicinal plants against human pathogens. Journal of Ethnopharmacology, 236, 331-340.

60) Omran, B. A., Rabbee, M. F., Abdel-Salam, M. O., & Baek, K. H. (2024). Biogenically synthesized copper oxide, titanium oxide, and silver oxide nanoparticles: Characterization and biological effects. Clean Technologies and Environmental Policy, 1-26.

61) Padinharayil, H., Varghese, J., John, M. C., Rajanikant, G. K., Wilson, C. M., Al-Yozbaki, M., ... & George, A. (2023). Non-small cell lung carcinoma (NSCLC): Implications on molecular pathology and advances in early diagnostics and therapeutics. Genes & Diseases, 10(3), 960-989.

62) Palanisamy, C. P., Poompradub, S., Sansanaphongpricha, K., Jayaraman, S., Subramani, K., & Sonsudin, F. (2025). Green synthesis of Nigella sativa-mediated silver nanoparticles for enhanced antibacterial activity and wound healing: Mechanistic insights and biomedical applications. Environmental Nanotechnology, Monitoring & Management, 101085.

63) Pan, E., Bogumil, D., Cortessis, V., Yu, S., & Nieva, J. (2020). A systematic review of the efficacy of preclinical models of lung cancer drugs. Frontiers in Oncology, 10, 591.

64) Pandey, P., Lakhanpal, S., Bishoyi, A. K., Jyothi, S. R., Mishra, S., Verma, M., ... & Khan, F. (2025). Biosynthesis of silver nanoparticles from plant extracts: a comprehensive review focused on anticancer therapy. Frontiers in Pharmacology, 16, 1600347.

65) Pathan, A., Nayak, T., Alshahrani, S., Tripathi, R., & Tripathi, P. (2025). Current and emerging frontiers in biologically synthesized gold nanoparticles: an in-depth review. Chemical Papers, 1-22.

66) Pei, Y., Clifford, C. A., & Minelli, C. (2025). Nanoparticle characterisation and standardisation. In Nanotechnology Tools for Infection Control (pp. 71-108). Elsevier.

67) Pirsaheb, M., Gholami, T., Seifi, H., Dawi, E. A., Said, E. A., Hamoody, A. H. M., ... & Salavati-Niasari, M. (2024). Green synthesis of nanomaterials by using plant extracts as reducing and capping agents. Environmental Science and Pollution Research, 31(17), 24768-24787.

68) Pleh, A., Mahmutović, L., & Hromić-Jahjefendić, A. (2021). Evaluation of phytochemical antioxidant levels by hydrogen peroxide scavenging assay. Bioengineering Studies, 2(1), 1-10.

69) Ponnusamy, A., Murugan, G., Mittal, A., Saetang, J., Prodpran, T., Rhim, J. W., & Benjakul, S. (2025). Carbon Dots Derived from Polyphenols by Hydrothermal Carbonization: Spectral, Antioxidant, and Antimicrobial Properties and Cytotoxicity Assessment. Food Biophysics, 20(2), 89.

70) Prieto, P., Pineda, M., & Aguilar, M. (1999). Spectrophotometric quantitation of antioxidant capacity through the formation of a phosphomolybdenum complex: specific application to the determination of vitamin E. Analytical biochemistry, 269(2), 337-341.

71) Quinson, J., Kunz, S., & Arenz, M. (2023). Surfactant-free colloidal syntheses of precious metal nanoparticles for improved catalysts. ACS Catalysis, 13(7), 4903-4937.

72) Rehman, N. U., Muhammad, G., Sharif, M. U., & Hussain, M. A. (2024). Green synthesis of silver nanoparticles using Lepidium sativum seed mucilage as a bioreductant/capping agent for efficient antibacterial and photocatalytic activities. Desalination and Water Treatment, 320, 100853.

73) Ritu, Verma, K. K., Das, A., & Chandra, P. (2023). Phytochemical-based synthesis of silver nanoparticle: mechanism and potential applications. BioNanoScience, 13(3), 1359-1380.

74) Roointan, A., Mir, T. A., Wani, S. I., Hussain, K. K., Ahmed, B., Abrahim, S., ... & Akhtar, M. H. (2019). Early detection of lung cancer biomarkers through biosensor technology: A review. Journal of pharmaceutical and biomedical analysis, 164, 93-103.

75) Sadiq, M. U., Shah, A., Haleem, A., Shah, S. M., & Shah, I. (2023). Eucalyptus globulus mediated green synthesis of environmentally benign metal based nanostructures: a review. Nanomaterials, 13(13), 2019.

76) Said, A. H., Shaibah, F., Moustafa, M., & Elamary, R. B. (2025). Plant-mediated nickel oxide nanoparticles show species-dependent antibacterial, antioxidant, anti-inflammatory and antidiabetic activities. Scientific Reports, 15(1), 31096.

77) Sati, A., Ranade, T. N., Mali, S. N., Ahmad Yasin, H. K., & Pratap, A. (2025). Silver nanoparticles (AgNPs): comprehensive insights into bio/synthesis, key influencing factors, multifaceted applications, and toxicity─ a 2024 update. ACS omega, 10(8), 7549-7582.

78) Sharma, B., Dhiman, C., Hasan, G. M., Shamsi, A., & Hassan, M. I. (2024). Pharmacological features and therapeutic implications of plumbagin in cancer and metabolic disorders: A narrative review. Nutrients, 16(17), 3033.

79) Sidhu, A. K., Verma, N., & Kaushal, P. (2022). Role of biogenic capping agents in the synthesis of metallic nanoparticles and evaluation of their therapeutic potential. Frontiers in Nanotechnology, 3, 801620.

80) Sikdar, S., & Sikdar, M. (2023). Green synthesis, optimization and analyzing of silver nanoparticles encapsulated with Syzygium aromaticum extract: Evaluating antibacterial and photocatalytic properties. Bioresource Technology Reports, 24, 101669.

81) Singaravelu, S., Motsoene, F., Abrahamse, H., & Dhilip Kumar, S. S. (2025). Green-synthesized metal nanoparticles: a promising approach for accelerated wound healing. Frontiers in bioengineering and biotechnology, 13, 1637589.

82) Singh, A., Banerjee, S. L., Gantait, A., Kumari, K., & Kundu, P. P. (2023). Metal-based nanoparticles: synthesis and biomedical applications. In Nanoparticles Reinforced Metal Nanocomposites: Mechanical Performance and Durability (pp. 365-408). Singapore: Springer Nature Singapore.

83) Spitzmüller, L., Berson, J., Schimmel, T., Kohl, T., & Nitschke, F. (2024). Temperature stability and enhanced transport properties by surface modifications of silica nanoparticle tracers for geo-reservoir exploration. Scientific Reports, 14(1), 19222.

84) Sreelekha, E., George, B., Shyam, A., Sajina, N., & Mathew, B. (2021). A comparative study on the synthesis, characterization, and antioxidant activity of green and chemically synthesized silver nanoparticles. BioNanoScience, 11(2), 489-496.

85) Thirumurugan, A., Padmanaban, M., Kumar, D. S., Govindharaju, R., Padmavathy, S., Karthikeyan, V., ... & Karthik, S. (2026). Phytochemical and antioxidant properties of Kedrostis foetidissima and its larvicidal potential against mosquitoes. South African Journal of Botany.

86) Upadhyay, P., Ghosh, A., Sarangthem, V., & Singh, T. D. (2024). Nanocarrier mediated co-delivery of phytochemicals and chemo-drugs: an emerging strategy to combat lung cancer in a systemic way. Phytochemistry Reviews, 23(2), 485-527.

87) Velmani, S., Sholkamy, E. N., Ruba, P., Kanaga, S., Balamurugan, V., Tarighat, M. A., & Abdi, G. (2025). Eco-friendly synthesis and biomedical potential of silver nanoparticles using Pandanus dubius extract. Scientific Reports, 15(1), 39940.

88) Vidjeyamannane, C., Joy, A., Prakash, K., & Saravanakumar, R. (2025). A comprehensive review on the role of plant-derived bioactive metabolites driving ROS-mediated apoptosis in cancer. Medical Oncology, 42(9), 1-16.

89) Vijayakumar, M., Priya, K., Nancy, F. T., Noorlidah, A., & Ahmed, A. B. A. (2013). Biosynthesis, characterisation and anti-bacterial effect of plant-mediated silver nanoparticles using Artemisia nilagirica. Industrial crops and products, 41, 235-240.

90) Vinoth, C., Ramya, J. R., Gajendiran, J., Gnanam, S., Raj, S. G., Kumar, G. R., & Karthikeyan, M. (2023). Structural, magnetic, antimicrobial and hemolysis properties of sol–gel derived iron manganese tri oxide (FeMnO3) nanostructures. Inorganic Chemistry Communications, 154, 110952.

91) Sandhiya T, Jeyabharathi S, Thirumurugan A. Exploration of Antimicrobial Drug Targets from Human Breast Milk Lactobacillus for the Control of Vaginal

Infections. Int J Drug Deliv Technol. 2026;16(7s): 924-933; DOI: 10.25258/ijddt.16.7s.98.

92) Manikandan T, Thirumurugan A, Pavithra S, Sakthivel V, Ramya G, Prabha A L, Molecular docking studies, phytochemical profiling, and antioxidant activity assessment of bioactive compounds derived from *Pogostemon benghalensis* Brum.f. Kunth..Int J Drug Deliv Technol. 2026;16(2s): 473-494; DOI: 10.25258/ijddt.16. 473- 494

93) Meda SSR, Joseph NM, Lakshmikanthan M, Ayyadurai T, Muthu S. Comparative Efficacy of Mandelic Acid Peel versus Topical Kojic Acid 2% in the Treatment of Periorbital Melanosis. Int J Drug Deliv Technol. 2026;16(15s): 118-123. DOI: 10.25258/ijddt.16.15s.14.

94) Meda SSR, Srinivasan VR, Lakshmikanthan M, Ayyadurai T, Muthu S. Topical Prostaglandin Analogues in Androgenetic Alopecia: A Systematic Review of Clinical Evidence. Int J Drug Deliv Technol. 2026;16(15s): 108-117. DOI: 10.25258/ijddt.16.15s.13.

95) Mohan, P. K., Krishna, T. A., Stephy, P. P., Krishna, T. A., Thirumurugan, A., & Annamalai, A. (2026). Stigmasterol as a Potential Anti-Urolithiatic Agent: In Vitro Evaluation and Computational Insights into Renal Targets. Systems Ethnopharmacology and Sustainable Bioresources, 100002.

96) Wani, A. K., Akhtar, N., Mir, T. U. G., Singh, R., Jha, P. K., Mallik, S. K., ... & Prakash, A. (2023). Targeting apoptotic pathway of cancer cells with phytochemicals and plant-based nanomaterials. Biomolecules, 13(2), 194.

97) Sakthivel V, Ilanthiraya S, Jeevanantham G, Aravindhan T, Priya K, Thirumurugan A, Larvicidal Activity Of Marine Macroalgae: A Comprehensive Review. Int J Drug Deliv Technol. 2026;16(4s): 908-917; DOI: 10.25258/ijddt.16.4s.106

98) Wankhede, S., Badule, A., Chaure, S., Damahe, A., Damahe, M., & Porwal, O. (2025). Challenges and strategies in prodrug design: A comprehensive review. Journal of Advanced Scientific Research, 16(06), 1-20.

99) Wittlinger, F., & Laufer, S. A. (2021). The pre-clinical discovery and development of osimertinib used to treat non-small cell lung cancer. Expert opinion on drug discovery, 16(10), 1091-1103.

100) Yusuf, A., Almotairy, A. R. Z., Henidi, H., Alshehri, O. Y., & Aldughaim, M. S. (2023). Nanoparticles as drug delivery systems: a review of the implication of nanoparticles' physicochemical properties on responses in biological systems. Polymers, 15(7), 1596.

101) Zhuang, J., Ma, Z., Li, N., Chen, H., Yang, L., Lu, Y., ... & Tang, B. Z. (2024). Molecular Engineering of Plasma Membrane and Mitochondria Dual-Targeted NIR-II AIE Photosensitizer Evoking Synergetic Pyroptosis and Apoptosis. Advanced Materials, 36(5), 2309488.